Electronic Supplementary Material (ESI) for CrystEngComm.

Supporting Information

Figure S1 shows the SEM images of α-Fe_2O_3 hexagonal rings synthesized by excess phosphate ions, 0.15 mM and 0.3 mM. It could be found that the axial length of these two samples were 122±18 nm and 224±35 nm respectively. With the concentration of phosphate ions increased, the axial length of the nanoring grew; this was different with the previous samples. It was speculated that the phosphate also plays the role of growth additives along [006] zone axis.

Some control experiments were also carried out to check the role that the sodium sulfate had played on the formation of the polyhedrons. The experiment was carried out with the concentration of phosphate ions fixing at 0.05 mM. Thus, with the concentration of sodium sulfate increased from 0.11 to 2.2 mM, the shape of the obtained hematite nanocrystal changed from icositetrahedron to hexagonal ring (Fig. S2). This illustrates that sulfate ions also plays an important role in the dissolution of Fe_2O_3 along the *c* axis ([006] zone axis). By varying the ratios of phosphate and sulfate ions to ferric ions, we were able to control the size and morphology of the Fe_2O_3 hexagonal ring.

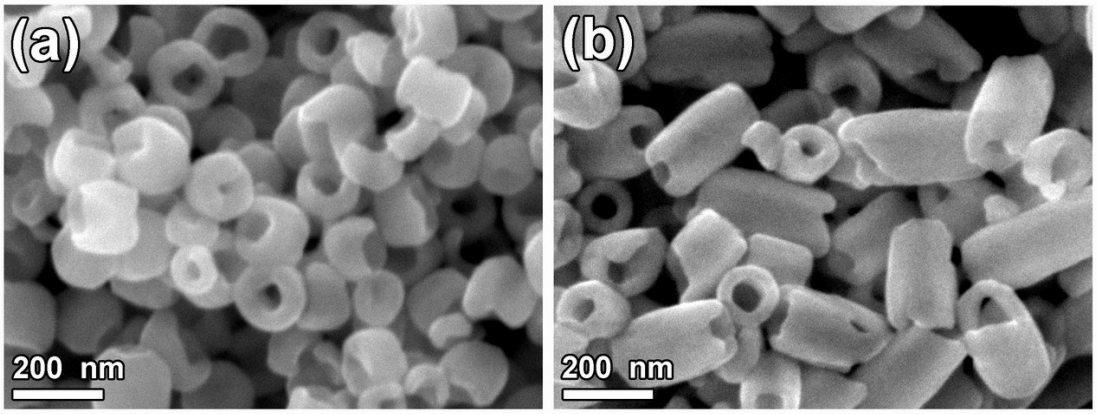

Figure S1. SEM images of α-Fe_2O_3 hexagonal rings synthesized by excess phosphate ions, (a) 0.15 mM, (b) 0.3 mM.

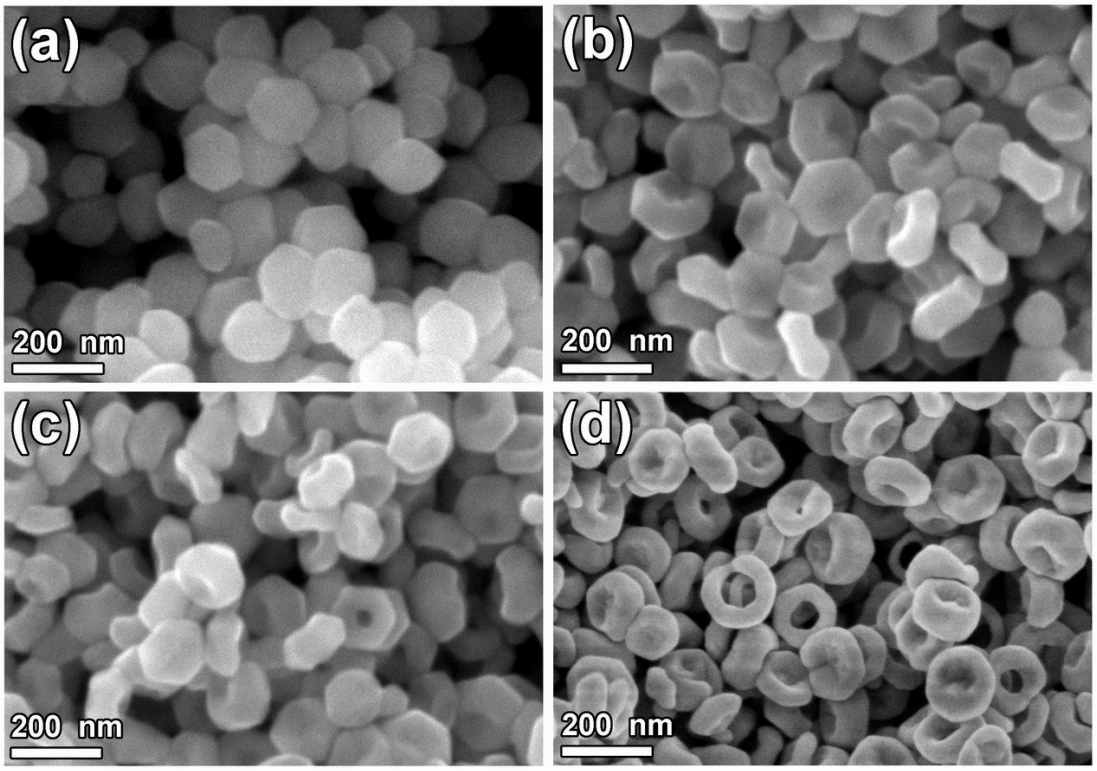

Figure S2. Shape evolution of the Fe_2O_3 polyhedrons with different concentration of sodium sulfate, (a) 0.11, (b) 0.55, (c) 1.1 and (d) 2.2 mM, by fixing the phosphate ions concentration at 0.05 mM.

To further prove the role of phosphate and sulfate ions in the formation process of the hematite polyhedrons, we did another two control experiments using sulfate or phosphate ions as the additive only. If we use the sulfate ions as the additive, the shape of the hematite products remain unchanged (Fig. S3a, b) with the concentration of the sulfate ions increased from 0.55 to 2.2 mM. When the phosphate ions were used as the only additive, with the concentration of the phosphate ions increased from 0.1 to 1.0 mM, the shape of the Fe_2O_3 nanocrystals evolved from icositetrahedron to short tube. These phenomena illustrate that in the evolution process of Fe_2O_3 icositetrahedron to concave nanocrystal and hexagonal ring, phosphate ions were the virtual etching agent. Sulfate ions had no direct corrosion effect, but as anions, they may act as capping agent instead of phosphate ions, and assist the corrosion behavior of the phosphate ions at the end of the Fe_2O_3 icositetrahedron.

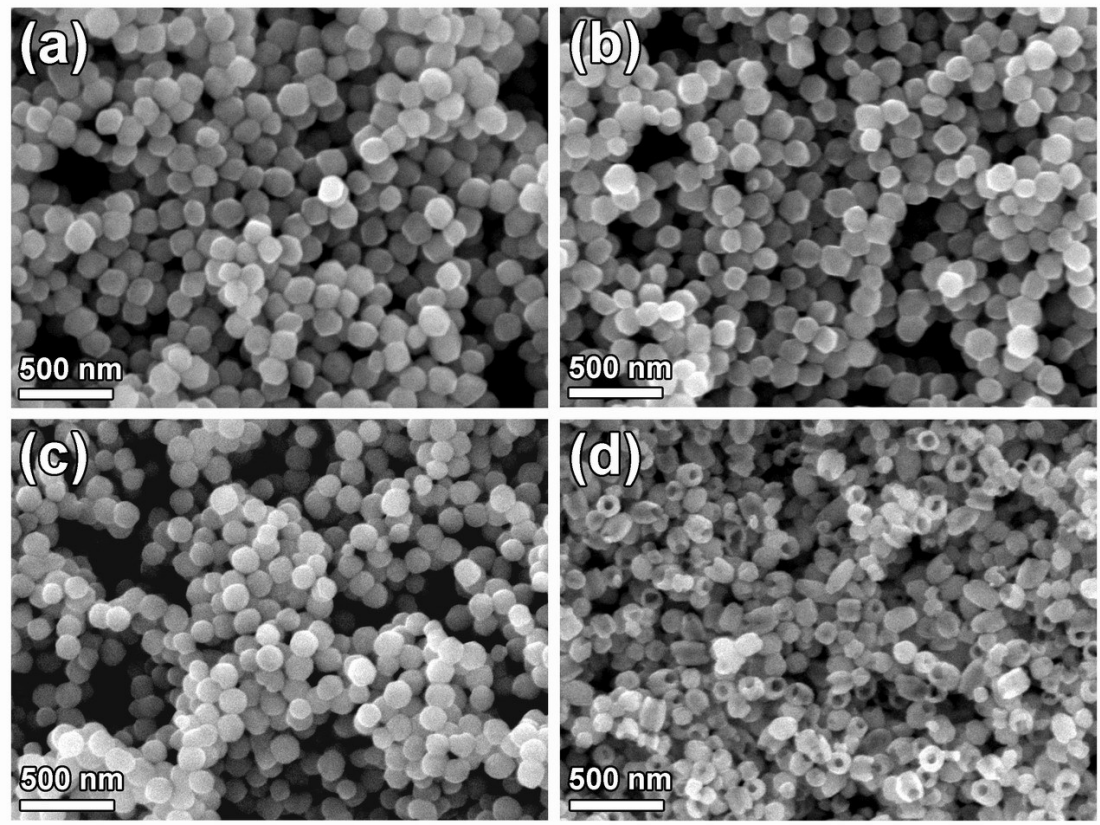

Figure S3. Control experiment using sulfate or phosphate ions as the additive only. (a, b) Sulfate ions were used as the only additive, the concentration of which was 0.55 and 2.2 mM; (c, d) Phosphate ions were the only additive, the concentration of which was 0.1 and 1.0 mM, respectively.

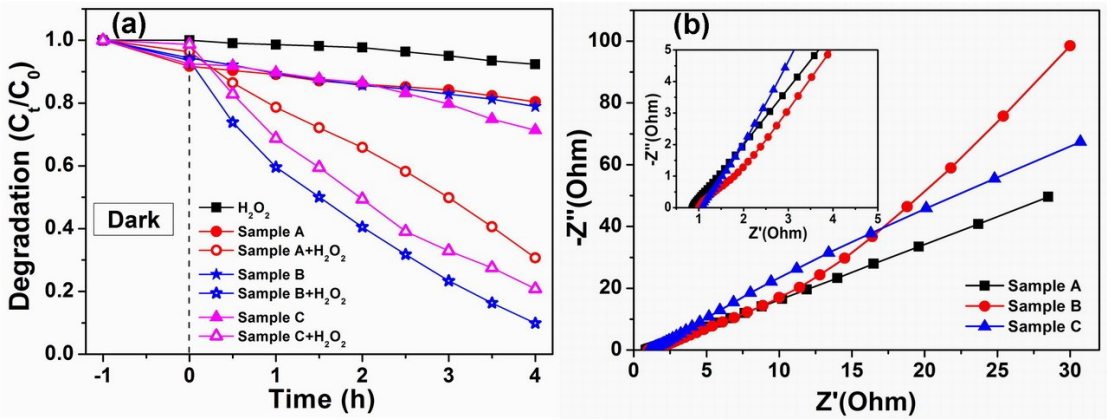

Figure S4. (a) The changes of the RhB relative concentrations (C/C0) as a function of irradiation time; (b) The EIS measurements were carried out to further evaluate the electrochemical behaviors of the three typical Fe_2O_3 polyhedrons.

For comparison, several control experiments were performed under similar conditions (Fig. S4a), including (1) dye + H_2O_2 (without Fe_2O_3 catalyst), (2) dye + Fe_2O_3 catalyst, (3) dye + H_2O_2 + Fe_2O_3 catalyst. However, in both situation (1) and (2), the (Photo) Fenton reaction were very slow, as compared to those obviously occurred

in condition (3) that α-Fe_2O_3 catalyst and H_2O_2 were used simultaneously. The results of the EIS measurements showed that the impedance spectra were composed of one semicircle at high frequency (inset of Fig. S4b) and a linear part at low frequency, illustrating a typical capacitor behavior. At the high frequency region, the intercept on the real axis which represents the equivalent series resistance (*Rs*) showed the sequence as: Sample C > Sample B > Sample A, in accordance with the specific surface area (SSA) order of the materials. At the low frequency region, the concave Fe_2O_3 polyhedron (Sample B) showed a more vertical curve, representing the fast ion diffusion in electrolyte and the adsorption onto the electrode surface.

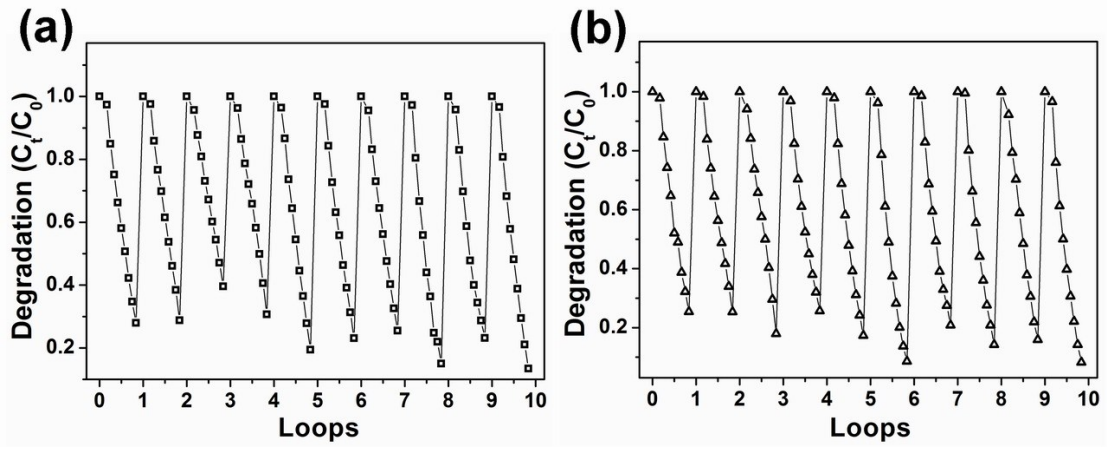

Figure S5. Recycling capability of Fe_2O_3 icositetrahedron (Sample A) and hexagonal ring (Sample C).

Figure S5 shows the recycling capability of Fe_2O_3 icositetrahedron (Sample A) and hexagonal ring (Sample C). During the 10 times recycling process of RhB degradation, the catalytic performance of these two samples almost remains stable. SEM images and XRD patterns of the three typical Fe_2O_3 polyhedrons before and after reused over 10 times on the degradation of RhB were shown in Figure S6. The results showed that after 10 times reaction, the morphology and crystallinity of the three typical Fe_2O_3 polyhedrons almost retained, only the surface of the samples changed a little roughness.

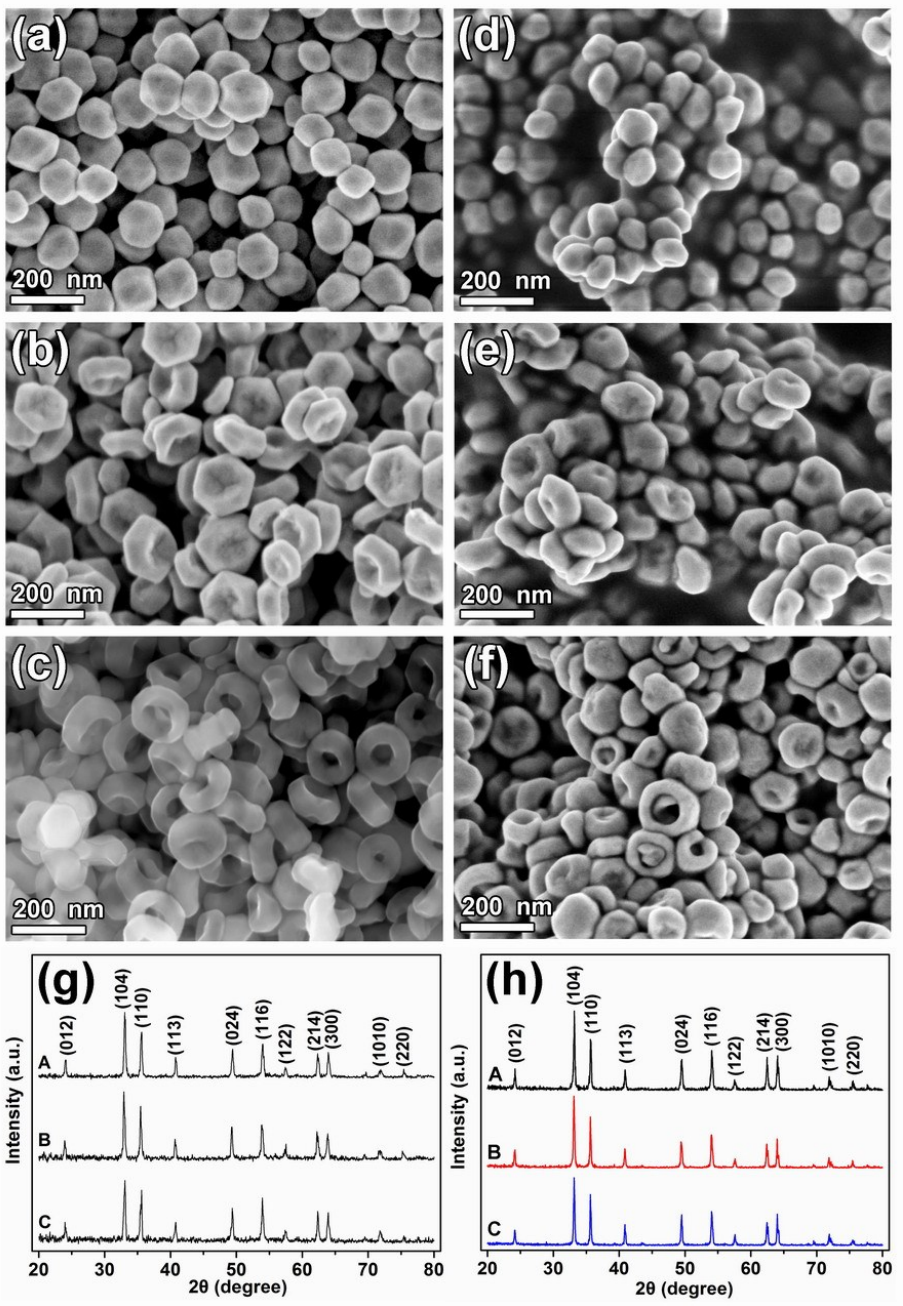

Figure S6. SEM images and XRD patterns of the three typical Fe_2O_3 polyhedrons before and after reused over 10 times on the degradation of RhB, (a-c) SEM images of icositetrahedron, concave and hexagonal ring of Fe_2O_3 polyhedrons before reused; (d-f) the according SEM images after reused 10 times; (g, h) XRD patterns of the Fe_2O_3 polyhedrons before and after reused over 10 times.